Characterization and stereochemistry of cofactor oxidation by a type II dihydrofolate reductase

ARTICLE *in* BIOCHEMISTRY · OCTOBER 1990

Impact Factor: 3.02 · DOI: 10.1021/bi00494a011 · Source: PubMed

Characterization and Stereochemistry of Cofactor Oxidation by a Type II Dihydrofolate Reductase†

Rui M. M. Brito,‡ Rebecca Reddick,‡ George N. Bennett,‡ Frederick B. Rudolph,‡ and Paul R. Rosevear*,§

Department of Biochemistry, Rice University, Houston, Texas 77005, and Department of Biochemistry and Molecular Biology, University of Texas Medical School at Houston, Houston, Texas 77225

Received May 18, 1990; Revised Manuscript Received July 24, 1990

ABSTRACT: Type II dihydrofolate reductases (DHFRs) encoded by the R67 and R388 plasmids are different both in sequence and in structure from known chromosomal DHFRs. These plasmid-derived DHFRs are responsible for conferring trimethoprim resistance to the host strain. A derivative of R388 DHFR, RBG200, has been cloned and overproduced [Vermersch, P. S., Klass, M. R., & Bennett, G. N. (1986) *Gene 41*, 289]. With this cloned and overproduced protein, a rapid purification procedure has been developed that yields milligram quantities of apparently homogeneous RBG200 DHFR with a specific activity 1.5-fold greater than that previously reported for the purified R388 protein [Amyes, S. G. B., & Smith, J. T. (1976) *Eur. J. Biochem. 61*, 597]. The pH versus activity profile and the native molecular weight of RBG200 DHFR were found to be similar to those previously reported for other type II DHFRs but different from those of the known chromosomal DHFRs. Stereospecifically labeled [4(*S*)-^{2}H,4(*R*)-^{1}H]NADPH was synthesized and used to determine the stereospecificity of NADPH oxidation by RBG200 DHFR. RBG200 DHFR was found to specifically transfer the *pro-R* hydrogen of NADPH to dihydrofolate, making it a member of the A-stereospecific class of dehydrogenases. Thus, although RBG200 DHFR is different both in sequence and in structure from known chromosomal enzymes, both enzymes catalyze identical hydrogen-transfer reactions. Two distinct binary RBG200 DHFR–NADP$^+$ complexes were detected by monitoring the ^{1}H NMR chemical shifts and line widths of the coenzyme in the presence of RBG200 DHFR. Addition of NADP$^+$ to the enzyme results in the formation of an initial binary complex (conformation I) which interconverts to a more stable binary complex (conformation II). At 25 °C the apparent first-order rate constant for the interconversion between conformations I and II was determined to be approximately 1.0×10^{-4} s^{-1}. Conformations I and II are characterized by upfield and downfield chemical shifts of the nicotinamide proton resonances from their positions in the free coenzyme, respectively. Changes in the ^{1}H NMR chemical shifts of the upfield-shifted methyl resonances of RBG200 DHFR were also observed upon NADP$^+$ binding and accompanying the interconversion between conformations I and II. The relevance of these two distinct binary conformations in coenzyme binding and catalysis remains to be determined.

Dihydrofolate reductase (DHFR;[1] EC 1.5.1.3) catalyzes a central reaction in one-carbon metabolism, the NADPH-dependent reduction of 7,8-dihydrofolate to 5,6,7,8-tetrahydrofolate. Chromosomal DHFRs are the target of a number of antifolate agents which function by inhibiting the enzyme and thus depleting the metabolic pool of one-carbon units necessary for normal cellular function. The discovery and use of the antifolate agents trimethoprim (TMP) and methotrexate (MTX) in clinical cases as antibacterial and antitumor agents led to the identification of different types of DHFRs, types I–IV, less sensitive to these antifolate compounds (Fleming et al., 1972; Amyes & Smith, 1974; Skold & Widh, 1974).

The type II enzymes were found to be specified by plasmids R67 and R388, which confer TMP resistance (Amyes & Smith, 1974; Pattishall et al., 1977). Isolation of type II enzymes and analysis of their enzymological properties showed them to be very insensitive to TMP and MTX, although they have K_m values for NADPH and dihydrofolate similar to those of the chromosomal enzymes (Pattishall et al., 1977). A comparison of the amino acid sequences of the R67- and R388-specified DHFRs showed homology over their 78 amino acid length. Of the 17 changes that occurred, 11 were from the N-terminus to amino acid 23, and two others were at the extreme C-terminus (Zolg et al., 1978; Zolg & Hanggi, 1981). This is in contrast to all known DHFRs from bacterial and mammalian sources which have been shown to be monomers of approximately 18 kDa (Kraut & Matthews, 1986).

The crystallographic structure of a dimeric form of R67 DHFR has been solved to 2.8-Å resolution (Matthews et al., 1986), although the active form of the enzyme appears to be a tetramer (Zolg & Hanggi, 1981; Smith et al., 1979). Crystallographic analysis of the dimer showed that each 78-residue subunit is folded into a 6-stranded antiparallel β-barrel. The β-strands from two subunits form a third β-barrel at the dimer interface. Matthews et al. (1986) have proposed that NADPH binds along a lengthwise cleft between the subunits. This structural motif suggests that the type II DHFRs have a pyridine nucleotide binding site different from those of chromosomal DHFRs and other known pyridine nucleotide binding proteins.

† This work was supported by National Science Foundation Grant DMB-8511026 to G.N.B., National Cancer Institute Grant 14030 to F.B.R., Army Research Office Grant DAAL-03-88-0069, and Grants from the Robert A. Welch Foundation (C-820, C-1041, and AU-1025 to G.N.B., F.B.R., and P.R.R., respectively).

* Author to whom correspondence should be addressed.

‡ Rice University.

§ University of Texas Medical School at Houston.

[1] Abbreviations: DHFR, dihydrofolate reductase; TMP, trimethoprim; MTX, methotrexate; DHF, 7,8-dihydrofolate; EDTA, ethylenediaminetetraacetic acid; DTT, 1,4-dithiothreitol; DSS, sodium 2,2-dimethyl-2-silapentane-5-sulfonate; SDS, sodium dodecyl sulfate; NMR, nuclear magnetic resonance; TLC, thin-layer chromatography; HPLC, high-pressure liquid chromatography; PMSF, phenylmethanesulfonyl fluoride.

0006-2960/90/0429-9825$02.50/0

A derivative of R388 DHFR, RBG200, having the sequence Thr-Thr-Ser-Arg-Thr-Leu- at the carboxy terminus in addition to the 78 amino acids of the R388 DHFR has been cloned and overproduced (Vermersch et al., 1986). A nondenaturing procedure for the rapid purification of milligram quantities of this derivative has been developed. RBG200 DHFR has been shown to have physical and chemical properties similar to those of the native R388 DHFR, making it an ideal system for biochemical studies aimed at elucidating the proposed novel mode of protein–cofactor interaction and the molecular basis for resistance to the common antifolate agents. With this purification procedure, RBG200 DHFR is soluble to at least 2 mM, making structural studies feasible. We have initiated biochemical studies required for a detailed understanding of the protein–cofactor interaction. The stereochemistry of hydride transfer from NADPH to DHF has been shown to be the same as that observed for chromosomal DHFRs. In addition, the existence of two distinct binary RBG200 DHFR–$NADP^+$ complexes has been observed by ^1H NMR spectroscopy.

Materials and Methods

Materials. Isocitrate dehydrogenase and $NADP^+$ were purchased from Sigma. ^2H_2O was purchased from Cambridge Isotope Laboratories. DEAE-Sepharose Fast Flow was purchased from Pharmacia. All other chemicals were of highest quality commericially available.

Enzyme Assay. Dihydrofolate reductase activity was assayed as described by Smith and Burchall (1983), except the buffer used was 50 mM potassium phosphate, 1 mM EDTA, and 1 mM DTT at pH 5.9. One enzyme unit is the quantity of enzyme required to convert 1 μmol of NADPH and dihydrofolate to $NADP^+$ and tetrahydrofolate per minute calculated on the basis of an absorption coefficient of 12 300 L mol^{-1} cm^{-1} at 340 nm (Smith & Burchall, 1983). Protein concentration was estimated by the method of Bradford (1976).

Bacterial Strains and Growth. Escherichia coli C600 cells bearing the plasmid RBG200 (Vermersch et al., 1986) were grown in minimal media in the presence of 0.2% casein amino acids and 15 mg/L trimethoprim. Cells were harvested by centrifugation, mixed with an equal weight of 50 mM Tris buffer containing 10% sucrose at pH 7.5, poured into liquid nitrogen, and stored at −70 °C.

Buffers. Cell lysis buffer contained 50 mM Tris, pH 8.0, 5% glycerol, 2 mM EDTA, 1 mM DTT, 0.24 M NaCl, 1.4 mM 2-mercaptoethanol, and 0.1 mM PMSF. TGED buffer is 10 mM Tris, pH 8.0, 5% glycerol, 0.1 mM EDTA, 0.2 M NaCl, 0.1 mM PMSF, and 1 mM DTT. TME buffer contained 10 mM Tris, pH 8.5, 10 mM 2-mercaptoethanol, and 1 mM EDTA. PMSF was added to the buffers immediately prior to use.

Purification of RBG200 DHFR. The following procedure is for 20 g of *E. coli* C600 cells bearing the plasmid pRBG200 DHFR. The basic steps consist of cell lysis, streptomycin sulfate precipitation, ammonium sulfate precipitation, and DEAE-Sepharose chromatography. All steps are carried out at 4 °C unless noted otherwise.

(*I*) *Cell Lysis.* Frozen cells, 20 g of frozen cell paste (1:1), are stirred at room temperature in 55 mL of lysis buffer until homogeneous. At 4 °C, 20 mg of lysozyme is added and the suspension stirred for 25 min. Freshly made 4% sodium deoxycholate is added to a final concentration of 0.1%; the solution is stirred an additional 2 min and incubated for an additional 20 min. To this solution, 55 mL of TGED buffer and 100 mL of 50 mM Tris-HCl, pH 7.5, containing 10 mM 2-mercaptoethanol are added with stirring, and the chromosomal DNA is sheared in a blender at medium speed for 30 s. The cell lysate is then centrifuged at 10000*g* for 45 min. The supernatant is fraction I.

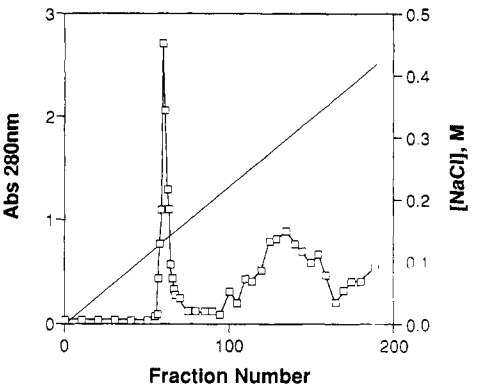

FIGURE 1: Ion exchange chromatography of RBG200 DHFR on DEAE-Sepharose. The dialyzed 35–50% ammonium sulfate fraction was applied to a 2.5 × 45 cm DEAE-Sepharose Fast Flow column equilibrated in TME buffer and washed in TME buffer. RBG200 DHFR was eluted with a 1.6-L gradient from 0 to 0.5 M NaCl in TME buffer. A flow rate of 40 mL/h was maintained throughout, and 8-mL fractions were collected. The RBG200 DHFR elutes at approximately 0.15 M NaCl with a specific activity of 2.8 units/mg.

(*II*) *Streptomycin Sulfate Precipitation.* Streptomycin sulfate is added dropwise to fraction I with constant stirring to a final concentration 1%. After complete addition of the streptomycin sulfate, the suspension is stirred for an additional 15 min and then centrifuged at 10000*g* for 15 min. The nucleic acid precipitate is discarded, and the supernatant, fraction II, is considered the crude extract.

(*III*) *Ammonium Sulfate Precipitation.* Solid ammonium sulfate is slowly added to fraction II with constant stirring over a 30-min period to 35% saturation. The suspension is stirred for 30 min and centrifuged at 10000*g* for 45 min. The precipitate is discarded, and solid ammonium sulfate is slowly added over a 30-min period to 50% saturation. After complete addition of the ammonium sulfate, the suspension is stirred for an additional 30 min. The ammonium sulfate precipitate is collected by centrifugation at 10000*g* for 45 min. The supernatant is discarded . The precipitate is dissolved in 20 mL of TME buffer and dialyzed twice against 3 L of TME buffer to give fraction III.

(*IV*) *DEAE-Sepharose Chromatography.* Fraction III is centrifuged at 10000*g* for 15 min and the supernatant loaded onto a 2.5 × 45 cm DEAE-Sepharose Fast Flow column equilibrated in TME buffer. After the supernatant has been loaded onto the column, the column is washed with 1 L of TME buffer. RBG200 DHFR is eluted with a 1.6-L linear gradient from 0 to 0.5 M NaCl in TME buffer. Dihydrofolate reductase elutes at approximately 0.15 M NaCl (Figure 1, fractions 55–66) with a specific activity of 2.8 units/mg (Table I). The purity of the enzyme was constant across the peak, as judged by SDS–polyacrylamide gel electrophoresis. An SDS–polyacrylamide gel of the pooled fraction from the DEAE-Sepharose column revealed one major band (>95%) corresponding to the known subunit molecular weight of RBG200 DHFR (Vermersch et al., 1986; Figure 2). The purified RBG200 DHFR was dialyzed against 5 mM potassium phosphate, pH 5.9, lyophilized, and stored at −20 °C with no measurable loss of activity over 3 months.

Determination of the Stereochemistry of NADPH Oxidation. [4-^2H]$NADP^+$ was prepared by alkaline cyanide treatment of $NADP^+$ in ^2H_2O according to the procedure of San Pietro (1955). ^1H NMR spectroscopy was used to confirm

Table I: Purification of RBG200 DHFR

	total protein (mg)	total act. (units)	sp act. (units/mg)	x-fold purification	% recovery
crude lysate	671	217	0.3		100
ammonium sulfate precipitation	378	206	0.5	1.7	95
DEAE-Sepharose	31	86	2.8	9.3	40

the position of the isotopic label and estimate the extent of deuteration (>95%). [4(*S*)-^{2}H,4(*R*)-^{1}H]NADPH was prepared with isocitrate dehydrogenase. The reaction mixture contained 50 mM Tris-HCl buffer at pH 7.2, 10 mM isocitric acid, 5 mM [4-^{2}H]NADP$^+$, 50 μM $MnSO_4$, and 2 units of isocitrate dehydrogenase in a final volume of 1.5 mL. The mixture was incubated for 2 h at 37 °C and the extent of reaction monitored by the increase in absorption at 340 nm. The reaction mixture was diluted to 50 mL with 10 mM triethylammonium bicarbonate buffer, pH 7.5, and loaded onto a 1.5 × 90 cm Pharmacia Fast Flow DEAE-Sepharose column equilibrated in 10 mM triethylammonium bicarbonate buffer, pH 7.5. The labeled NADPH was eluted with a 500-mL linear gradient from 10 to 500 mM triethylammonium bicarbonate, pH 7.5, at a flow rate of 1.5 mL/min. Fractions having A_{260}/A_{340} ratios of approximately 2.5 were pooled, and the isotopically labeled NADPH precipitated with a 10-fold excess of cold acetone. The chemical shift and coupling constant of the C4 methylene proton of the isotopically labeled NADPH confirmed the stereochemistry at C4 to be 4(*S*)-^{2}H,4(*R*)-^{1}H. The [4(*S*)-^{2}H,4(*R*)-^{1}H]NADPH (70 μM) was incubated with RBG200 DHFR (0.11 mg) in a reaction mixture which contained 45 mM potassium phosphate buffer, pH 5.9, 120 μM dihydrofolate, and 12 mM 2-mercaptoethanol for 1 h at 22 °C. The reaction mixture was diluted with 50 mL of 10 mM triethylammonium bicarbonate buffer, pH 7.5, and loaded onto a 1.5 × 30 cm Pharmacia Fast Flow DEAE-Sepharose column. NADP$^+$ was eluted with a 500-mL linear gradient from 10 to 500 mM triethylammonium bicarbonate, pH 7.5. Fractions containing the purified NADP$^+$ were pooled, and the NADP$^+$ was collected by precipitation with a 10-fold excess of cold acetone. The precipitated NADP$^+$ was dissolved in ^2H_2O for analysis by ^{1}H NMR. The stereochemistry of oxidation of [4(*S*)-^{2}H,4(*R*)-^{1}H]NADPH by RBG200 DHFR was not monitored continuously in the NMR spectrometer due to interference by dihydrofolate, tetrahydrofolate, and aromatic amino acid residues of the protein. Proton NMR spectra were obtained at 22 °C on a GN500 NMR spectrometer. Spectra were obtained by collecting 128 transients with 16K data points, a spectral width of 5000 Hz, a 90° pulse, and a 5-s repetition rate. DSS was used as an internal standard and the pH of the samples adjusted to 7.0.

Enzyme Preparation for NMR Studies. Purified RBG200 DHFR, from a lyophilized powder, was dissolved in 50 mM potassium phosphate buffer, pH 6.0, in ^2H_2O. The solution was lyophilized and redissolved in ^2H_2O to remove most of the residual HDO and to deuterate exchangeable protons. All buffer and reagent solutions used in the NMR studies were treated with Chelex 100 before use to remove trace metal contaminants. RBG200 DHFR was found to retain at least 90% of its original activity at the end of the NMR experiments.

Results and Discussion

Purification of RBG200 DHFR. The purification procedure for RBG200 DHFR from *E. coli* C600 cells carrying the plasmid pRBG200 is summarized in Table I, and the SDS–polyacrylamide gel electrophoresis monitoring the purification from crude extracts is shown in Figure 2. The overall purification from 10 g of cell paste (20 g of 1:1 mixture of cells and Tris/sucrose buffer) is 31 mg of apparently homogeneous enzyme, representing a 40% yield. The specific activity of RBG200 DHFR, 2.8 units/mg, is significantly higher than the specific activity previously reported for the similar R388 enzyme, 1.5 units/mg (Zolg & Hanggi, 1981). The increased specific activity of RBG200 DHFR, a derivative of the R388 enzyme, most likely results from the more gentle and rapid purification procedure used to purify the overproduced protein. The previous purification procedure included a step where the enzyme is denatured by boiling in 6 M guanidinium chloride and passed over a gel filtration column in 6 M urea (Zolg & Hanggi, 1981). RBG200 DHFR purified according to the procedure of Zolg and Hanggi (1981) was also found to have a lower specific activity, approximately 1.5 units/mg. Thus, it is possible that once the type II DHFR is partially unfolded it does not refold completely to its native conformation. Preliminary circular dichroism studies of RBG200 DHFR at pH 5.9 show a significant amount of α-helical structure, in contrast to the antiparallel β-sheet structure obtained by crystallography for the dimeric form of R67 DHFR (Matthews et al., 1986).

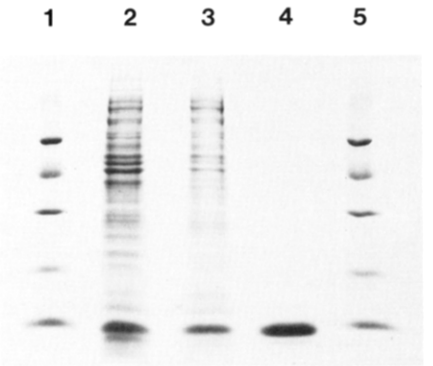

FIGURE 2: The 20% SDS–polyacrylamide gel electrophoresis monitoring the purification of RBG200 DHFR from *E. coli* C600 cells carrying the plasmid RBG200. (Lanes 1 and 5) Molecular mass standards: bovine serum albumin (68 kDa), hen egg albumin (45 kDa), soybean trypsin inhibitor (20.1 kDa), and α-lactalbumin (14.2 kDa). (Lane 2) Supernatant from streptomycin sulfate precipitation. (Lane 3) Dialyzed fraction from the 35–50% ammonium sulfate cut. (Lane 4) RBG200 DHFR eluted from the DEAE-Sepharose column. The gel was stained with Coomassie Brilliant Blue.

With the overproduction of RBG200 DHFR and the simplified purification scheme, large amounts of RBG200 DHFR can be prepared for biochemical and NMR studies aimed at understanding the unique structural properties of this protein. In addition, this type of purification scheme is necessary before efficient incorporation of stable isotopes into RBG200 DHFR becomes practical for detailed magnetic resonance studies. A major advantage of RBG200 DHFR is its greatly increased solubility (>2 mM) compared to that of the R67 or R388 proteins.

pH Profile of RBG200 DHFR. The pH versus activity profile of RBG200 DHFR is shown in Figure 3. RBG200 DHFR has a sharp pH optimum at 5.9, similar to that observed for the R388 enzyme (Amyes & Smith, 1976). At pH 7.5 the enzyme exhibits approximately 25% of its maximal activity. However, at pH 5.0, less than 1 pH unit from the pH of maximal activity, RBG200 DHFR exhibits only 5% of

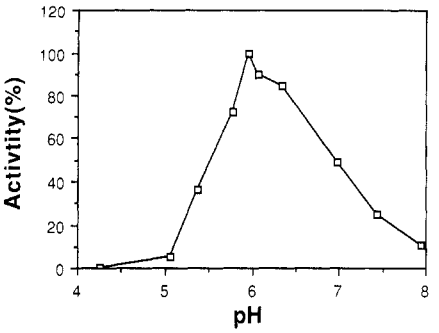

FIGURE 3: pH versus activity profile for RBG200 DHFR. The percentage of RBG200 DHFR activity is shown at different pH values. Potassium phosphate buffer, 50 mM, containing 1 mM EDTA and 1 mM DTT was used for the pH range 4.2–7.9. The pH was measured prior to, and immediately after, monitoring of the absorbance change of reaction with a microelectrode and found to vary less than ±0.05 unit. Each data point is the average of three separate assays.

its maximal activity. The sharp decrease in activity over approximately 0.9 pH unit may result from protonation of a carboxylate group essential in catalysis or in maintaining the proper quaternary or tertiary structure of the enzyme. This is in contrast with the *E. coli* chromosomal DHFR which exhibits a broad pH optimum between pH 5.5 and pH 7.5 (Matthews & Sutherland, 1965; Amyes & Smith, 1976).

Native Molecular Mass of RBG200 DHFR. The native molecular mass of the purified enzyme was determined at both pH 5.9 and pH 5.0 by HPLC gel filtration on a Superose 12 column (Figure 4). RBG200 DHFR yielded a single peak with an apparent molecular mass of 32 and 35 kDa at pH 5.9 and 5.0, respectively (Figure 4). From the subunit molecular mass, 8.8 kDa (Vermersch et al., 1986), the native enzyme exists in solution as a tetramer at both pH values. This is consistent with the subunit composition previously found for the R67 enzyme (Smith et al., 1979). Thus, it appears that type II plasmid derived DHFRs are tetramers composed of four identical subunits, in contrast with all known chromosomal DHFRs which exist as monomers with molecular masses of approximately 18 kDa (Smith et al., 1979). Gel filtration experiments at pH 5.0 (Figure 4B) also demonstrate that RBG200 DHFR maintains its quaternary structure at low pH and rapid loss of enzymatic activity between pH 5.9 and pH 5.0 (Figure 3) is not the result of dissociation of the active enzyme into inactive monomers or dimers.

Hydride-Transfer Stereospecificity of RBG200 DHFR. [4(*S*)-^{2}H,4(*R*)-^{1}H]NADPH was synthesized from [4-^{2}H]-NADP$^+$ with isocitrate dehydrogenase and isocitric acid. It is well established that isocitrate dehydrogenase transfers a hydrogen from the C2 of isocitric acid to the A face (*pro-R* position) of NADPH (Englard & Colowick, 1957; Nakamoto & Vennesland, 1960; Freudenthal et al., 1973). Additionally, the stereochemistry and isotopic purity of the synthesized NADPH were confirmed by ^{1}H NMR spectroscopy (Arnold et al., 1976; Seyama et al., 1977; Arnold & You, 1978).

The synthesized [4(*S*)-^{2}H,4(*R*)-^{1}H]NADPH was incubated with dihydrofolate and RGB200 DHFR, and the enzymatically oxidized NADPH was isolated by column chromatography. This was necessary to prevent interference in the ^{1}H NMR spectrum of NADP$^+$ from the protein, NADPH, dihydrofolate, and tetrahydrofolate. If the type II plasmid DHFR transferred the A-side (*pro-R*) hydrogen, the isolated NADP$^+$ would contain deuterium at the N4 position. However, if the enzyme transferred the B-side (*pro-S*) hydrogen, the isolated NADP$^+$ would contain a proton at the N4 position. The ^{1}H NMR spectra of the aromatic region of commercial NADP$^+$ and NADP$^+$ isolated from incubation of [4(*S*)-^{2}H,4(*R*)-^{1}H]-NADPH with RBG200 DHFR are compared in Figure 5. The isolated NADP$^+$ is shown to contain deuterium at N4 (Figure 5A). Therefore, RBG200 DHFR specifically removes the *pro-R* hydrogen, leaving behind the *pro-S* deuterium. Chromosomal DHFRs are known to transfer the *pro-R* hydrogen from NADPH to dihydrofolate (Charlton et al., 1979). Thus, the stereochemistry of hydrogen transfer from NADPH to dihydrofolate by two evolutionary distinct reductases is identical. This was predicted to be a general rule by Colowick et al. (1966) and shown to be correect for evolutionarily divergent sources of L-lactate dehydrogenase and malate dehydrogenase, both A-stereospecific enzymes (Arnold et al., 1976).

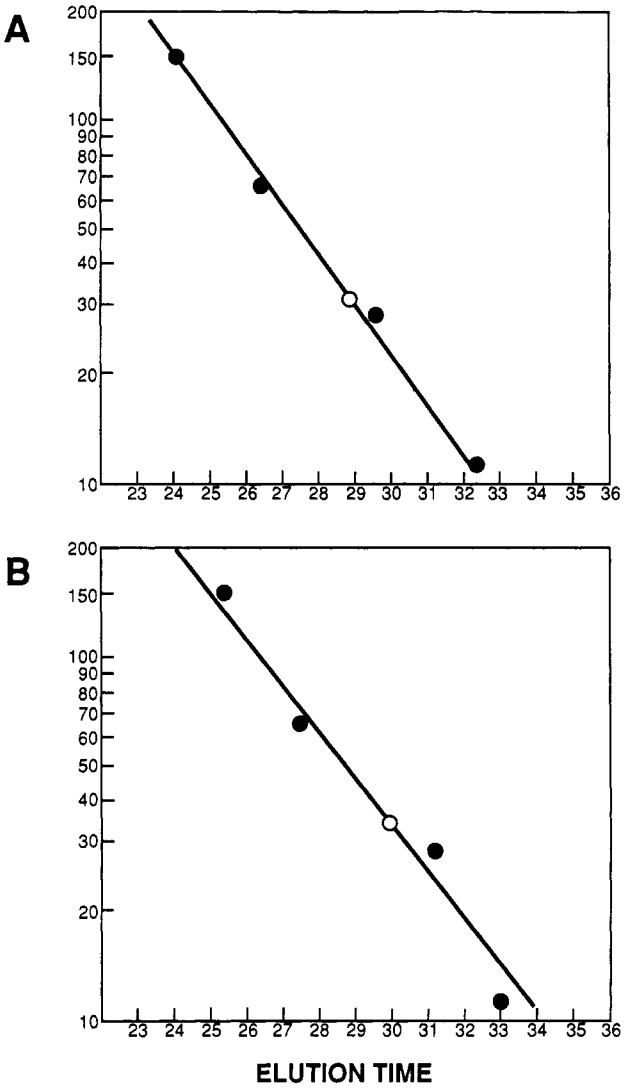

FIGURE 4: Estimation of the native molecular mass of purified RBG200 DHFR at pH 5.9 (A) and pH 5.0 (B). Gel filtration was performed on a Superose 12 (Pharmacia) HPLC column, 10 × 300 mm, at 25 °C in 50 mM potassium phosphate buffer, pH 5.9, containing 50 mM NaCl (A) or in 50 mM potassium phosphate buffer, pH 5.0, containing a 50 mM NaCl (B). A flow rate of 0.5 mL/min was used at both pH values. A calibration curve was prepared with the following molecular mass standards (●): alcohol dehydrogenase (150 kDa), bovine serum albumin (68 kDa), carbonic anhydrate (29 kDa), and cytochrome *c* (12.4 kDa). Native RBG200 DHRF (○) eluted at a position corresponding to a molecular mass of 32 (A) and 35 kDa (B), respectively.

NMR experiments using the chromosomal DHFR and [4-^{2}H]NADPH have previously shown that hydride ion transfer is to the C6 *si* face of the pteridine ring in dihydrofolate, producing the biologically active isomer of tetrahydrofolate (Pastore & Friedkin, 1962). Under the growth conditions

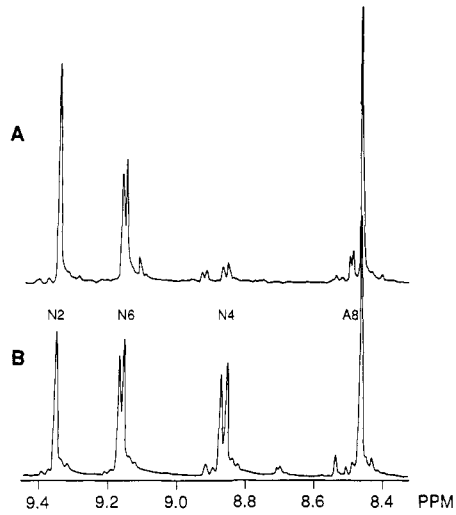

FIGURE 5: Comparison of the aromatic region of the 500-MHz ^1H NMR spectrum of (A) $NADP^+$ isolated from the oxidation of [4-(*R*)-^1H,4(*S*)-^2H]NADPH by RBG200 DHFR and (B) commercial $NADP^+$. The nicotinamide protons are labeled N2, N6, and N4. The adenine H8 proton is labeled A8.

utilized, *E. coli* strain C600 will not grow in the presence of trimethoprim without the plasmid carrying the gene for RBG200 DHFR (Vermersch et al., 1986). Therefore, the only source of tetrahydrofolate in the presence of trimethoprim is that synthesized by the type II DHFR encoded by the plasmid RBG200. Since the tetrahydrofolate synthesized by RBG200 DHFR is necessary for cell growth and only the C6 *si* isomer of tetrahydrofolate is biologically active (Charlton et al., 1979; Fontecilla-Champs et al., 1979), RBG200 DHFR is transferring the C4 *pro-R* hydrogen of NADPH to the C6 *si* face of the pteridine ring in dihydrofolate.

Evidence for Two Interconverting RBG200 DHFR–$NADP^+$ Complexes in Solution. Figure 6 shows the nicotinamide HN2 and HN6 protons of 5 mM $NADP^+$ in the presence of 0.5 mM RBG200 DHFR as a function of time at 25 °C. The presence of enzyme caused extensive broadening and upfield chemical shifts of both nicotinamide resonances (Figure 6B). Chemical shift changes and line broadening for the adenine and ribose resonances of $NADP^+$ were also observed immediately upon addition of RBG200 DHFR (data not shown). A second set of nicotinamide proton resonances were also observed downfield of the exchange-broadened resonances having chemical shifts closer to those of the free coenzyme (Figure 6B,E). After incubation of $NADP^+$ with RBG200 DHFR at 25 °C for 1 h, two distinct sets of HN2 and HN6 proton resonances are more clearly observed (Figure 6C). Continued incubation for 10.5 h results in the observation of just a single set of HN2 and HN6 proton resonances (Figure 6D) with chemical shifts closer to those of the free coenzyme (Figure 6E). This behavior is consistent with the slow time-dependent conformational interconversion between two distinct binary RBG200 DHFR–$NADP^+$ complexes. In the initial conformation, conformation I, the nicotinamide portion of the coenzyme is in an environment which produces upfield chemical shifts of 0.021 and 0.049 ppm in the HN2 and HN6 protons, respectively. The chemical shift changes in the nicotinamide proton resonances indicate that the oxidized nicotinamide ring does interact with RBG200 DHFR in a highly specific manner. In contrast, the chemical shift changes on coenzyme binding to the final binary conformation, conformation II, are smaller, 0.011 ppm, for both HN2 and HN6 and downfield from the resonances of the free coenzyme. The line broadening of the HN2 and HN6 resonances in conformation I, compared with

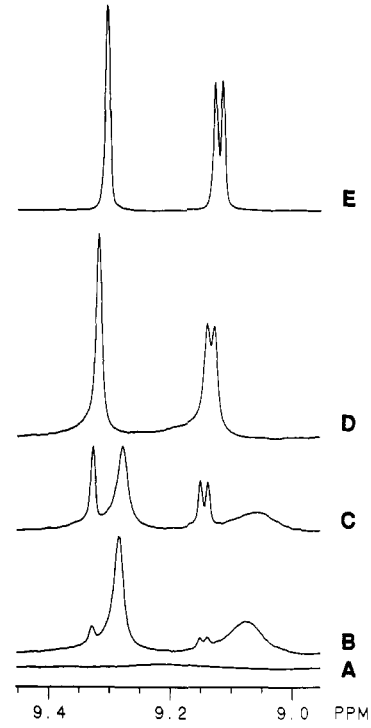

FIGURE 6: HN2 and HN6 proton resonances of 5 mM $NADP^+$ in the presence of 0.5 mM RBG200 DHFR at 25 °C showing the time-dependent interconversion from the initial binary RBG200 DHFR–$NADP^+$ complex (conformation I) to the final binary complex (conformation II). (A) Aromatic proton region of RBG200 DHFR in the absence of $NADP^+$; (B) nicotinamide HN2 and HN6 protons of 5 mM $NADP^+$ immediately after addition of 0.5 mM RBG200 DHFR; (C) proton NMR spectrum of the aromatic region after 1-h incubation with RBG200 DHFR showing two sets of HN2 and HN6 proton resonances of the coenzyme; (D) proton NMR spectrum of the aromatic region after 10.5-h incubation with RBG200 DHFR showing the HN2 and HN6 protons of the coenzyme in the final binary RBG200 DHFR–$NADP^+$ complex; (E) nicotinamide HN2 and HN6 protons of free $NADP^+$ in solution under identical conditions. NMR spectra were obtained at 500 MHz by use of 32 transients with 16K data points, a spectral width of 7042 Hz, a recycle time of 3 s, and a line broadening of 2 Hz.

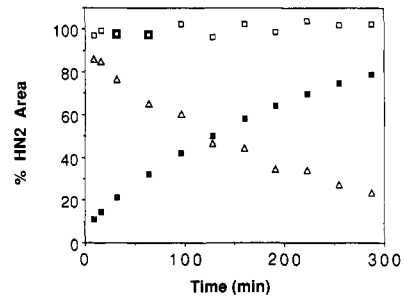

FIGURE 7: Kinetics of interconversion at 25 °C of RBG200 DHFR–$NADP^+$ conformation I to conformation II by monitoring of the integral of nicotinamide HN2 resonance in both complexes. The reaction contained 5 mM $NADP^+$ and 0.5 mM RBG200 DHFR in 50 mM potassium phosphate buffer in ^2H_2O, pH 5.9. Area of the HN2 resonance in conformation I (△). Area of the HN2 resonance in conformation II (■). Sum of the area of HN2 in both conformation I and conformation II (□).

that in conformation II, implies that the dissociation of $NADP^+$ in conformation I is slower than in conformation II. The rate of interconversion of conformation I to conformation II was determined by measuring the area of the HN2 resonance in both conformations I and II as a function of time (Figure 7). Figure 7 shows the decrease in area of the HN2 resonance in conformation I with the corresponding increase in area of the HN2 resonance in conformation II. The total intensity of the HN2 resonance from both conformations I and

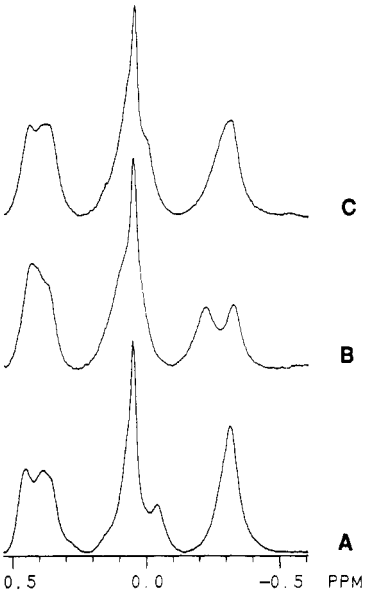

FIGURE 8: NMR spectra of the upfield-shifted methyl resonances in RBG200 DHFR showing the effect of $NADP^+$ addition and the time-dependent interconversion from conformation I to conformation II. The sample contained 0.5 mM RBG200 DHFR in 50 mM potassium phosphate buffer in ^2H_2O at pH 5.9. (A) Upfield-shifted methyl region of RBG200 DHFR in the absence of $NADP^+$. (B) Upfield-shifted methyl region of RBG200 DHFR 9 min after the addition of 5 mM $NADP^+$. (C) Upfield-shifted methyl region of RBG200 DHFR 10.5 h after the addition of $NADP^+$. NMR spectra were obtained under the conditions described in Figure 6.

II remained constant throughout the time course of the interconversion, indicating that a two-state model of the interconversion process is adequate (Figure 7). From the data in Figure 7, an apparent first-order rate constant of 1.0×10^{-4} s^{-1} at 25 °C was found for the interconversion of conformation I to conformation II. At 5 °C an apparent first-order rate constant of 9.3×10^{-6} s^{-1} for this interconversion was determined (data not shown). From the apparent first-order rate constants, an energy of activation E_a = 20 kcal/mol was estimated. The activation rate parameters estimated for the interconversion are $\Delta H^{\ddagger}$ = 33 kcal/mol, $\Delta S^{\ddagger}$ = 34 cal/(mol·deg), and $\Delta G^{\ddagger}$ = 23 kcal/mol (at 25 °C). These values are in the range of those observed for the conformational interconversion of two distinct chromosomal *Lactobacillus casei* DHFR–trimethoprim–$NADP^+$ ternary complexes (Gronenborn et al., 1981a,b).

The binding of $NADP^+$ and the formation of the initial binary complex (conformation I) can also be detected by monitoring the chemical shifts of the upfield-shifted methyl resonances of RBG200 DHFR (Figure 8). Comparison of the upfield-shifted methyl regions of RBG200 DHFR in the absence of (Figure 8A) and immediately after addition of $NADP^+$ (Figure 8B) reveals several chemical shift changes in the methyl resonances upon addition of coenzyme and formation of binary conformation I. After 10.5 h, time sufficient for complete interconversion of conformation I to conformation II, a different pattern of chemical shifts for the methyl resonances is observed for the complex in conformation II (Figure 8C). This pattern is more similar to that found for enzyme alone. However, the line widths of the methyl resonances are broader than those found for enzyme alone due to an exchange contribution from the binding of $NADP^+$. Although conformational changes in the protein observed upon interconversion of the two complexes cannot yet be described in detail, alterations in the upfield-shifted methyl protons are most simply explained by altered geometric relationships of the methyl groups to aromatic rings of either the protein or coenzyme. Chemical shift changes observed in this region are consistent with the formation of an initial binary RBG200 DHFR–$NADP^+$ complex, involving an initial conformational alteration in the protein, which slowly converts to a second binary complex in which the coenzyme or the protein exists in a different environment or conformation. The existence of two or more conformational states has been detected in ternary complexes of chromosomal *L. casei* DHFR–trimethoprim–$NADP^+$, but not in binary complexes with $NADP^+$ (Hyde et al., 1980; Gronenborn et al., 1981a,b).

Conclusions. A rapid and gentle purification procedure for RBG200 DHFR, a cloned and overproduced derivative of R388 DHFR having the sequence Thr-Thr-Ser-Arg-Thr-Leu at the carboxy terminus, has been developed which yields milligram quantities of apparently homogeneous protein with a specific activity 1.5-fold greater than that previously reported for the R388 protein (Amyes & Smith, 1976). The active form of RBG200 DHFR was found to be a tetramer in solution with a pH optimum near 5.9. RBG200 DHFR, a type II dihydrofolate reductase, has been shown to stereospecifically transfer the *pro-R* proton of NADPH to dihydrofolate, making it a member, along with chromosomal dihydrofolate reductases, of the A-stereospecific class of dehydrogenases. NMR studies monitoring the proton chemical shifts of $NADP^+$ upon addition of RBG200 DHFR have permitted the detection of two distinct binary RBG200 DHFR–$NADP^+$ complexes in solution. The nature of the conformational states and their structural/functional role in catalysis remain to be determined. Studies are in progress to elucidate the structural differences between these two complexes in order to better understand their role in coenzyme binding and activity. The ability to rapidly prepare large quantities of RGB200 DHFR will facilitate physical and structural studies aimed at understanding the unique mode of cofactor interaction with this novel dihydrofolate reductase.

ACKNOWLEDGMENTS

We thank Dr. N. J. Openheimer for useful discussions.

REFERENCES

Amyes, S. G. B., & Smith, J. T. (1974) *Biochem. Biophys. Res. Commun. 58*, 412.

Amyes, S. G. B., & Smith, J. T. (1976) *Eur. J. Biochem. 61*, 597.

Arnold, L. J., & You, K. (1978) *Methods Enzymol. 54*, 223.

Arnold, L. J., You, K., Allison, W. S., & Kaplan, N. O. (1976) *Biochemistry 15*, 4844.

Bradford, M. M. (1976) *Anal. Biochem. 72*, 248.

Charlton, P. A., Young, D. W., Birdsall, B., Feeney, J., & Roberts, G. C. K. (1979) *J. Chem. Soc., Chem. Commun.*, 922.

Colowick, S., van Eys, J., & Park, J. H. (1966) in *Comprehensive Biochemistry* (Florkin, M., & State, E. H., Eds.) Vol. 14, p 1, Elsevier, Amsterdam.

Englard, S., & Colowick, S. P. (1957) *J. Biol. Chem. 226*, 1047.

Fleming, M. P., Datta, N., & Gruneburg, R. N. (1972) *Br. Med. J. 1*, 726.

Fontecilla-Camps, J. C., Bugg, C. E., Temple, C., Jr., Rose, J. D., Montgomery, J. A., & Kisliuk, R. L. (1979) *J. Am. Chem. Soc. 101*, 6114.

Freudenthal, R. I., Kepler, J. A., & Cook, C. E. (1973) *Anal. Chem. 51*, 632.

Gornall, A. G., Bardawill, C. J., & David, M. M. (1949) *J. Biol. Chem. 177*, 751.

Gronenborn, A., Birdsall, B., Hyde, E. I., Roberts, G. C. K., Fenney, J., & Burgen, A. S. V. (1981a) *Nature 290*, 273.
Gronenborn, A., Birdsall, B., Hyde, E. I., Roberts, G. C. K., Feeney, J., & Burgen, A. S. V. (1981b) *Mol. Pharmacol. 20*, 145.
Hitchings, G. H., & Smith, S. L. (1980) *Adv. Enzyme Regul. 18*, 349.
Hyde, E. I., Birdsall, B., Roberts, G. C. K., Feeney, J., & Burgen, A. S. V. (1980) *Biochemistry 19*, 3738.
Kraut, J., & Matthews, D. A. (1986) in *Biological Macromolecules and Assemblies* (Journak, F., & McPherson, A., Eds.) Vol. III, Wiley, New York.
Matthews, C. K., & Sutherland, K. E. (1965) *J. Biol. Chem. 240*, 2142.
Matthews, D. A., Smith, S. L., Baccarani, D. P., Burchall, J. J., Oatley, S. J., & Kraut, J. (1986) *Biochemistry 25*, 4194.
Nakamoto, T., & Vennesland, B. (1960) *J. Biol. Chem. 235*, 202.
Pastore, E. J., & Friedkin, M. (1962) *J. Biol. Chem. 237*, 3802.
Pattishall, K. H., Acar, J., Burchall, J. J., Goldstein, F. W., & Harvey, R. J. (1977) *J. Biol. Chem. 252*, 2319.
San Pietro, A. (1955) *J. Biol. Chem. 217*, 579.
Seyama, Y., Kasama, T., Yamakawa, T., Kawaguchi, A., & Okuda, S. (1977) *J. Biochem. 81*, 1167.
Skold, O., & Widh, A. (1974) *J. Biol. Chem. 249*, 4324.
Smith, S. L., & Burchall, J. J. (1983) *Proc. Natl. Acad. Sci. U.S.A. 80*, 4619.
Smith, S. L., Stone, D., Novak, P., Baccanari, D. P., & Burchall, J. J. (1979) *J. Biol. Chem. 254*, 6222.
Vermersch, P. S., Klass, M. R., & Bennett, G. N. (1986) *Gene 41*, 289.
Zolg, J. W., & Hanggi, U. J. (1981) *Nucleic Acids Res. 9*, 697.
Zolg, J., Hanggi, U., & Zachau, H. (1978) *Mol. Gen. Genet. 164*, 15.

Reactivity of Parallel-Stranded DNA to Chemical Modification Reagents

Jan Klysik,‡ Karsten Rippe, and Thomas M. Jovin*

Department of Molecular Biology, Max Planck Institute for Biophysical Chemistry, Postfach 2841, D-3400 Göttingen, FRG

Received May 2, 1990; Revised Manuscript Received July 20, 1990

ABSTRACT: Four 25-nt long oligonucleotides containing dA and dT (D1, D2, D3, and D4) which are capable of forming parallel-stranded (ps) or antiparallel-stranded (aps) duplexes have been synthesized [Rippe, K., Ramsing, N. B., & Jovin, T. M. (1989) *Biochemistry 28*, 9536–9541]. In the present study, the OsO_4–pyridine complex (Os,py), diethyl pyrocarbonate (DEPC), $KMnO_4$, and the 1,10-phenanthroline–cuprous complex [$(OP)_2Cu^+$] were used to investigate the conformation-dependent reactivity of ps, aps, and single-stranded (ss) oligonucleotides. The products were analyzed by polyacrylamide gel electrophoresis with single-nucleotide resolution. The results confirm the duplex nature of the ps combinations of oligonucleotides and reveal structural differences in comparison with the aps molecules. Under conditions in which ss-DNA is substantially sensitive to Os,py, both the ps and aps duplexes are very unreactive. A similar result was observed with $KMnO_4$ and DEPC, although with the latter reagent the modification pattern of the labeled strands D1* and D4* was slightly different for the parallel than for the antiparallel duplex. The $(OP)_2Cu^+$ complex efficiently cleaves the aps but not the ps duplex and shows a preference for TAT steps. We also tested the effect of monovalent and divalent cation concentrations on the chemical reactivity of the ps, aps, and ss species. Elevated NaCl concentration leads to a dramatic increase in the Os,py and $KMnO_4$ modification of ss molecules and the ps, but not the aps, duplex. We attribute the apparent reaction with ps-DNA to a destabilization of this conformation under the conditions of reaction. In contrast, all reactions with DEPC are somewhat depressed at high salt concentration. The effects of $MgCl_2$ and temperature on the chemical reactivity with Os,py were also determined. The helix–coil transition of both the ps and the aps duplexes can be monitored by chemical modification with the OsO_4–pyridine reagent.

The antiparallel orientation of DNA strands is a characteristic feature of all right-handed B-type and left-handed Z-type helices. In 1986, N. Pattabiraman presented force field calculations indicating the possibility that a stable duplex composed of $d(A)_6$ and $d(T)_6$ could form with both strands oriented in the same 5′–3′ direction and associated via *reverse* Watson–Crick base pairing with the glycosidic bonds in a trans orientation (Pattabiraman, 1986). The calculated stability was similar to that of conventional antiparallel DNA, encouraging numerous experimental approaches for examining the existence and properties of parallel-stranded hairpins (van de Sande et al., 1988; Ramsing et al., 1989; Germann et al., 1989; Shchyolkina et al., 1989; Tchurikov et al., 1989) and of parallel-stranded duplexes (Ramsing & Jovin, 1988; German et al., 1988; Ramsing et al., 1989; Rippe et al., 1989, 1990; Rippe & Jovin, 1989; Jovin et al., 1990). On the basis of the results available to date, it is clear that DNA can adopt a parallel-stranded (ps)[1] conformation that is only moderately

‡Present address: Department of Biochemistry, University of Alabama, Birmingham, AL.
* Author to whom correspondence should be addressed.

0006-2960/90/0429-9831$02.50/0